

⁷Li NMR Studies on Complexation Reactions of Lithium Ion with Cryptand C211 in Ionic Liquids: Comparison with Corresponding Reactions in Nonaqueous Solvents

Atsushi Shirai and Yasuhisa Ikeda*

Research Laboratory for Nuclear Reactors, Tokyo Institute of Technology, 2-12-1-N1-34 O-okayama, Meguro-ku, Tokyo 152-8550, Japan

Received August 19, 2010

⁷Li NMR spectra of DEME-TFSA [DEME = *N,N*-diethyl-*N*-methyl-*N*-(2-methoxyethyl)ammonium; TFSA = bis-(trifluoromethanesulfonyl)amide], EMI-TFSA (EMI = 1-ethyl-3-methylimidazolium), MPP-TFSA (MPP = *N*-methyl-*N*-propylpyridinium), DEME-PFSA [PFSA = bis(pentafluoroethanesulfonyl)amide], and DEME-HFSA [HFSA = bis(heptafluoropropanesulfonyl)amide] ionic liquid (IL) solutions containing LiX (X = TFSA, PFSA, or HFSA) and C211 (4,7,13,18-tetraoxa-1,10-diazabicyclo[8.5.5]eicosane) were measured at various temperatures. As a result, it was found that the uncomplexed Li(I) species existing as [Li(X)₂][−] in the present ILs exchange with the complexed Li(I) ([Li·C211]⁺) and that the exchange reactions proceed through the bimolecular mechanism, [Li·C211]⁺ + [Li(X)₂][−] → [Li·C211]⁺ + [Li(X)₂][−]. Kinetic parameters [*k*_s/(kg m^{−1} s^{−1}) at 25 °C, Δ*H*[‡]/(kJ mol^{−1}), Δ*S*[‡]/(J K^{−1} mol^{−1})] are as follows: 5.57 × 10^{−2}, 69.8 ± 0.4, and −34.9 ± 1.0 for the DEME-TFSA system; 5.77 × 10^{−2}, 70.6 ± 0.2, and −31.9 ± 0.6 for the EMI-TFSA system; 6.13 × 10^{−2}, 69.0 ± 0.3, and −36.7 ± 0.7 for the MPP-TFSA system; 1.35 × 10^{−1}, 65.2 ± 0.5, and −43.1 ± 1.4 for the DEME-PFSA system; 1.14 × 10^{−1}, 64.4 ± 0.3, and −47.1 ± 0.6 for the DEME-HFSA system. To compare these kinetic data with those in conventional nonaqueous solvents, the exchange reactions of Li(I) between [Li·C211]⁺ and solvated Li(I) in *N,N*-dimethylformamide (DMF) and dimethyl sulfoxide (DMSO) were also examined. These Li(I) exchange reactions were found to be independent of the concentrations of the solvated Li(I) and hence proposed to proceed through the dissociative mechanism. Kinetic parameters [*k*_s/s^{−1} at 25 °C, Δ*H*[‡]/(kJ mol^{−1}), Δ*S*[‡]/(J K^{−1} mol^{−1})] are as follows: 1.10 × 10^{−2}, 68.9 ± 0.2, and −51.3 ± 0.4 for the DMF system; 1.13 × 10^{−2}, 76.3 ± 0.3, and −26.3 ± 0.8 for the DMSO system. The differences in reactivities between ILs and nonaqueous solvents were proposed to be attributed to those in the chemical forms of the uncomplexed Li(I) species, i.e., the negatively charged species ([Li(X)₂][−]) in ILs, and the positively charged ones ([Li(solvent)_n]⁺) in nonaqueous solvents.

1. Introduction

In recent years, ionic liquids (ILs) have been given attention as environmentally benign alternatives to conventional organic solvents because of their attractive properties such as thermal stability, nonflammability, high ionic conductivity, and wide electrochemical potential windows.^{1–3} In fact, applications of ILs to various fields, e.g., media for syntheses of organic compounds,^{4–7} extraction media for metal ions

(Mⁿ⁺),^{8–21} and electrolytes for capacitors or batteries,^{22–31} have been investigated.

In order to develop such applications, especially separations of Mⁿ⁺ using ILs as extraction media, data on the solvation and reactivity of metal complexes in ILs are necessary. However, limited information is available on the dynamic properties such as ligand exchange or substitution reactions of metal complexes in ILs and the solvent effects on their reactions. To our knowledge, only the following reactions have been reported, that is, the substitution reactions of [Pt(apa)Cl]⁺ [apa = 2,6-bis(aminomethyl)pyridine]

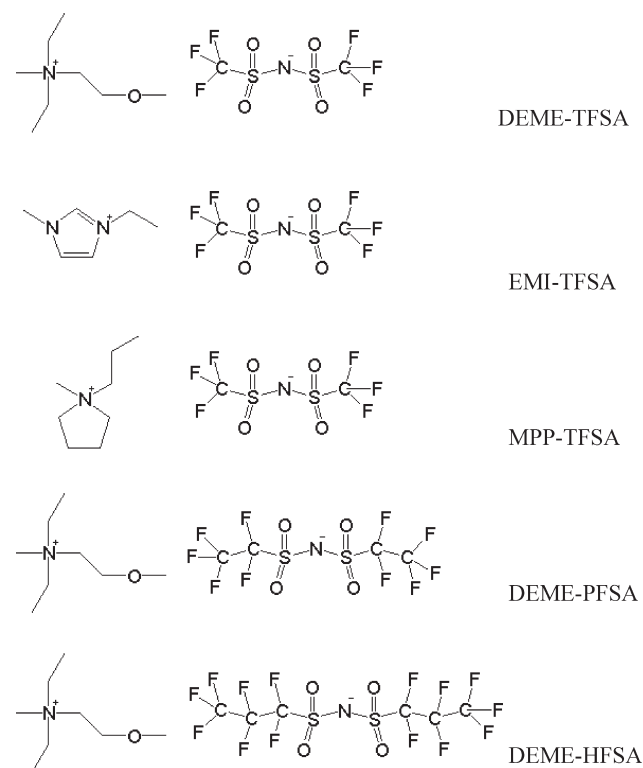
*To whom correspondence should be addressed. E-mail: yiked@nrr.titech.ac.jp. Phone: +81 3-5734-3061.

- (1) Earle, K. J.; Seddon, K. R. *Pure Appl. Chem.* **2000**, *72*, 1391.
- (2) *Green Industrial Applications of Ionic Liquids*; Rogers, R. D., Seddon, K. R., Volkov, S., Eds.; Kluwer Academic Publishers: Dordrecht, The Netherlands, 2000.
- (3) *Ionic Liquids in Synthesis*; Wasserscheid, P., Welton, T., Eds.; Wiley-VCH: New York, 2003.
- (4) Welton, T. *Chem. Rev.* **1999**, *99*, 2071–2083.
- (5) Wasserscheid, P.; Keim, W. *Angew. Chem., Int. Ed.* **2000**, *39*, 3772–3789.
- (6) Earle, M. J.; Katdare, S. P.; Seddon, K. R. *Org. Lett.* **2004**, *6*, 707–710.
- (7) Greaves, T. L.; Drummond, C. J. *Chem. Rev.* **2008**, *108*, 206–237.

- (8) Visser, A. E.; Swatoski, R. P.; Reichert, W. M.; Griffin, S. T.; Rogers, D. D. *Ind. Eng. Chem. Res.* **2000**, *39*, 3596–3604.
- (9) Chun, S.; Dzyuba, S. V.; Bartsch, R. A. *Anal. Chem.* **2001**, *73*, 3737–3741.
- (10) Jensen, M. P.; Neufeind, J.; Beitz, J. V.; Skanthakumar, S.; Soderholm, L. *J. Am. Chem. Soc.* **2003**, *125*, 15466–15473.
- (11) Wei, G.; Yang, Z.; Chen, C. *Anal. Chim. Acta* **2003**, *488*, 183–192.
- (12) Luo, H.; Dai, S.; Bonnesen, P. V. *Anal. Chem.* **2004**, *76*, 2773–2779.
- (13) Luo, H.; Dai, S.; Bonnesen, P. V.; Buchanan, A. C.; Holbrey, J. D.; Bridges, N. J.; Rogers, R. D. *Anal. Chem.* **2004**, *76*, 3078–3083.

with thiourea and iodide in 1-butyl-3-methylimidazolium bis(trifluoromethanesulfonyl)amide (BMI-TFSA),³² the substitution reactions of $[\text{Pt}(\text{ppp})\text{Cl}]^+$ ($\text{ppp} = 2,2':6',2''$ -terpyridine) with thiourea and thiocyanate in 1-ethyl-3-methylimidazolium (EMI)-based ILs,^{33,34} the reversible binding reaction of NO to $(\text{TMPS})\text{Fe}(\text{OH})$ ($\text{TMPS} = \text{meso}$ -[tetrakis(3-sulfonatomesityl)porphyrin]) in EMI-TFSA,³⁵ the complexation reactions of Li(I) with cryptand C211 in DEME-TFSA [DEME = *N,N*-diethyl-*N*-methyl-*N*-(2-methoxyethyl)ammonium],³⁶ and the OPPh_3 (triphenylphosphine oxide) exchange reaction of $[\text{UO}_2(\text{OPPh}_3)_4]^{2+}$ in BMI-NfO (NfO = nonafluorobutanesulfonate).³⁷ Most of these studies have examined whether the reactions of metal complexes in ILs proceed in a manner similar to those in the conventional solvents. Eldik et al. have found that the rates of substitution reactions in Pt(II) complexes in ILs are considerably slower than those in the corresponding reactions in methanol or water^{33,34} and suggested that a likely reason is the interaction between the anionic component of ILs and the positively charged metal complex. We also observed that the kinetic parameters [$7.2 \times 10^3 \text{ M}^{-1} \text{ s}^{-1}$ ($\text{M} = \text{mol dm}^{-3}$) at 25°C , $\Delta H^\ddagger = 55.3 \text{ kJ mol}^{-1}$, and $\Delta S^\ddagger = 16.1 \text{ J K}^{-1} \text{ mol}^{-1}$] for the OPPh_3 exchange reaction of $[\text{UO}_2(\text{OPPh}_3)_4]^{2+}$ in BMI-NfO are largely different from those ($1.4 \times 10^5 \text{ M}^{-1} \text{ s}^{-1}$ at 25°C , $\Delta H^\ddagger = 7.1 \text{ kJ mol}^{-1}$, and $\Delta S^\ddagger = -122 \text{ J K}^{-1} \text{ mol}^{-1}$) in CD_2Cl_2 ³⁷ and proposed that this difference is

Scheme 1. Schematic Structures of ILs Used in This Study



due to the specific solvation of NfO^- around $[\text{UO}_2(\text{OPPh}_3)_4]^{2+}$ through Coulombic interaction between the charged species.

As mentioned above, data on the reactivities of metal complexes in ILs have not been obtained sufficiently. Hence, as part of the acquisition of basic data on the reactivities of metal complexes in ILs, we have studied exchange reactions of Li(I) between the Li(I) complexed with cryptand C211 (4,7,13,18-tetraoxa-1,10-diazabicyclo[8.5.5]icicosane) and the uncomplexed Li(I) in DEME-TFSA, EMI-TFSA, MPP-TFSA (MPP = *N*-methyl-*N*-propylpyridinium), DEME-PFSA [PFSA = bis(pentafluoroethanesulfonyl)amide], and DEME-HFSA [HFSA = bis(heptafluoropropanesulfonyl)amide] (see Scheme 1) using a ^7Li NMR line-broadening method to examine the effect of anionic and cationic components in ILs. Furthermore, although some studies on the complexation reactions of Li(I) with cryptand in nonaqueous solvents have been reported,^{38–47} we have studied the exchange reactions of Li(I) between the Li(I) complexed with cryptand C211 and the solvated Li(I) in *N,N*-dimethylformamide

(14) Nakashima, K.; Kubota, F.; Maruyama, T.; Goto, M. *Ind. Eng. Chem. Res.* **2005**, *44*, 4367–4372.

(15) Zhao, H.; Xia, S.; Ma, P. *J. Chem. Technol. Biotechnol.* **2005**, *80*, 1089–1096.

(16) Stepinski, D. C.; Jensen, M. P.; Dzielawa, J. A.; Dietz, M. L. *Green Chem.* **2005**, *7*, 151–158.

(17) Nishii, N.; Murakami, H.; Imakura, S.; Kakiuchi, T. *Anal. Chem.* **2006**, *78*, 5805–5812.

(18) Pandey, S. *Anal. Chim. Acta* **2006**, *556*, 38–45.

(19) Kozono, N.; Ikeda, Y. *Monatsh. Chem.* **2007**, *138*, 1145–1151.

(20) Yuan, L.; Peng, J.; Xu, L.; Zhai, M.; Li, J.; Wei, G. *J. Phys. Chem. B* **2009**, *113*, 8948–8952.

(21) Egorov, V. M.; Djigailo, D. I.; Momotenko, D. S.; Chernyshov, D. V.; Torocheshnikova, I. I.; Smirnova, S. V.; Pletnev, I. V. *Talanta* **2010**, *80*, 1177–1182.

(22) Sato, T.; Masuda, G.; Takagi, K. *Electrochim. Acta* **2004**, *49*, 3603–3611.

(23) Sato, T.; Maruo, T.; Marukane, S.; Takagi, K. *J. Power Sources* **2004**, *138*, 253–261.

(24) Lee, S.-Y.; Yong, H. H.; Lee, Y. J.; Kim, S. K.; Ahn, S. *J. Phys. Chem. B* **2005**, *109*, 13663–13667.

(25) Shin, J.-H.; Henderson, W. A.; Appetecchi, G. B.; Alessandrini, F.; Passerini, S. *Electrochim. Acta* **2005**, *50*, 3859–3865.

(26) Hatayashi, K.; Nemoto, Y.; Akuto, K.; Sakurai, Y. *J. Power Sources* **2005**, *146*, 689–692.

(27) Seki, S.; Kobayashi, Y.; Miyashiro, H.; Ohno, Y.; Usami, A.; Mita, Y.; Kihira, N.; Watanabe, M.; Terada, N. *J. Phys. Chem. B* **2006**, *110*, 10228–10230.

(28) Matsumoto, H.; Sakaebe, H.; Tatsumi, K.; Kikuta, M.; Ishiko, E.; Kono, M. *J. Power Sources* **2006**, *160*, 1308–1313.

(29) Ferrari, S.; Quartarone, E.; Mustarelli, P.; Magistris, A.; Protti, S.; Lazzaroni, S.; Fagnoni, M.; Albini, A. *J. Power Sources* **2009**, *194*, 45–50.

(30) Lewandowski, A.; Swiderska-Moczek, A. *J. Power Sources* **2009**, *194*, 601–609.

(31) Hassoun, J.; Fernicola, A.; Navarra, M. A.; Panero, S.; Scrosati, B. *J. Power Sources* **2010**, *195*, 574–579.

(32) Weber, C. F.; Puchta, R.; van Eikema Hommes, N. J. R.; Wasserscheid, P.; van Eldik, R. *Angew. Chem., Int. Ed.* **2005**, *44*, 6033–6038.

(33) Begel, S.; Illner, P.; Kern, S.; Puchta, R.; van Eldik, R. *Inorg. Chem.* **2008**, *47*, 7121–7132.

(34) Illner, P.; Begel, S.; Kern, S.; Puchta, R.; van Eldik, R. *Inorg. Chem.* **2009**, *48*, 588–597.

(35) Schmeisser, M.; van Eldik, R. *Inorg. Chem.* **2009**, *48*, 7466–7475.

(36) Shirai, A.; Ikeda, Y. *Chem. Lett.* **2008**, *37*, 552–553.

(37) Takao, K.; Takahashi, T.; Ikeda, Y. *Inorg. Chem.* **2009**, *48*, 1744–1754.

(38) Cahen, Y. M.; Dye, J. L.; Popov, A. I. *J. Phys. Chem.* **1975**, *79*, 1289–1291.

(39) Cahen, Y. M.; Dye, J. L.; Popov, A. I. *J. Phys. Chem.* **1975**, *79*, 1292–1295.

(40) Shamsipur, M.; Popov, A. I. *J. Phys. Chem.* **1986**, *90*, 5997–5999.

(41) Lincoln, S. F.; Abou-Hamdan, A. *Inorg. Chem.* **1990**, *29*, 3584–3589.

(42) Shamsipur, M.; Karkhaneei, E.; Afkhami, A. *Polyhedron* **1998**, *17*, 3809–3815.

(43) Ceraso, J. M.; Smith, P. B.; Landers, J. S.; Dye, J. L. *J. Phys. Chem.* **1977**, *81*, 760–765.

(44) Lincoln, S. F.; Brereton, I. M.; Spotswood, T. M. *J. Chem. Soc., Faraday Trans. 1* **1985**, *81*, 1623–1630.

(45) Lincoln, S. F.; Brereton, I. M.; Spotswood, T. M. *J. Am. Chem. Soc.* **1986**, *108*, 8134–8138.

(46) Mei, E.; Popov, A. I.; Dye, J. L. *J. Am. Chem. Soc.* **1977**, *99*, 6532–6536.

(47) Shamsipur, M.; Popov, A. I. *J. Phys. Chem.* **1987**, *91*, 447–451.

(DMF) and dimethyl sulfoxide (DMSO) dissolving LiTfSA to compare with the reaction behavior in ILs.

2. Experimental Section

Materials. DEME-TfSA (Kanto Chemical Co., Inc.), EMI-TfSA (Japan Carlit Co., Ltd.), and MPP-TfSA (Kanto) were purified by stirring with active carbon in water for 72 h, followed by filtration of active carbon. A small amount of water in these ILs was removed by evaporation in vacuo at 80 °C for more than 72 h. Lithium bis(trifluoromethanesulfonyl)amide (LiTfSA) was prepared by neutralization of HTFAS (Kanto) with Li_2CO_3 (Kanto, 99.95%) in an aqueous solution, followed by evaporation of water. Lithium bis(pentafluoroethanesulfonyl)amide (LiPFSA; Kishida Chemical Co., Ltd., 99.5%) and LiHFSA (Wako, 99%) were dried by evaporation in vacuo at 80 °C for more than 72 h. The DEMECI compound was prepared by using the same method as that reported previously.⁴⁸ Cryptand C211 (Merck, 95%) was dried in vacuo at room temperature for 3 days and used without further purification. DMSO (Wako Pure Chemical Ind., Ltd.) and DMF (Kanto) were dried by storage over 4A molecular sieves (Wako) for 1 week. All other chemicals were of reagent grade and were used as received.

Syntheses of DEME-PFSA and DEME-HFSA. These hydrophobic ILs were synthesized according to an anion metathesis method described in previous papers.^{49,50} Each aqueous solution (ca. 100 mL) containing LiPFSA ($29.7 \text{ g}, 7.67 \times 10^{-2} \text{ mol}$) and LiHFSA ($30.2 \text{ g}, 6.19 \times 10^{-2} \text{ mol}$) was added slowly to aqueous solutions (ca. 100 mL) containing DEMECI ($13.8 \text{ g}, 7.60 \times 10^{-2} \text{ mol}$; $11.1 \text{ g}, 6.13 \times 10^{-2} \text{ mol}$), followed by stirring for 24 h at room temperature and separation of the DEME-PFSA and DEME-HFSA phases. In order to remove residual LiCl in the obtained DEME-PFSA and DEME-HFSA, the ultrapure water (ca. 200 mL) was added to CH_2Cl_2 solutions containing crude DEME-PFSA and DEME-HFSA, followed by shaking and standing. Furthermore, ultrapure water (ca. 200 mL) was added to the separated CH_2Cl_2 phase, followed by shaking and separation. These procedures were repeated seven times. To confirm the removal of LiCl in IL phases, the content of Li^+ and Cl^- ions in the aqueous phases obtained in every treatment was measured by using an inductively coupled plasma atomic emission spectrometer (PerkinElmer OPTIMA 3000) and an ion chromatograph (Dionex ICS-1500). After evaporation of water and CH_2Cl_2 in ILs, organic impurities were removed by stirring active carbon as mentioned above. Finally, the resulting DEME-PFSA and DEME-HFSA were dried by evaporation in vacuo at room temperature for more than 72 h.

Measurement of the Water Content of ILs. The water content of each dried IL was determined by a Karl Fischer titration method (Metrohm 831 KF coulometer), i.e., 6.5 ppm for DEME-TfSA, 11.6 ppm for EMI-TfSA, 6.3 ppm for MPP-TfSA, 6.5 ppm for DEME-PFSA, and 11.7 ppm for DEME-HFSA.

Measurements of NMR spectra of ILs. ^1H , ^{13}C , and ^{19}F NMR spectra of purified ILs were measured using JEOL JNM-LA300WB (^1H , 300.40 MHz) and JEOL ECX-400 FT-NMR (^{13}C , 100.53 MHz; ^{19}F , 376.17 MHz) spectrometers. Chemical shifts of ^1H and ^{13}C NMR were measured using tetramethylsilane as an internal standard, and those of ^{19}F NMR were determined using a D_2O solution containing 0.05 M NaF as an external reference. As a result, each IL was confirmed to be a single component (see Figures S1–S5 in the Supporting Information).

Kinetic Analyses of Exchange Reactions. Sample solutions for kinetic studies were prepared by dissolving LiTfSA, LiPFSA, or LiHFSA and appropriate amounts of C211 into ILs in a dry globebox. Kinetic analyses were carried out using a ^7Li NMR line-broadening method.⁵¹ ^7Li NMR spectra of sample solutions were measured using a JEOL-JNM-LA300WB (^7Li , 116.65 MHz) NMR spectrometer at various temperatures. The apparent first-order rate constants (k_{obs}) for the Li(I) exchange reactions were obtained from τ_{Li} values ($k_{\text{obs}} = 1/\tau_{\text{Li}}$), which are the mean lifetimes of Li(I) of the complexed site. The τ_{Li} values were evaluated from the best fitting of ^7Li NMR line shapes or obtained from the line width ($k_{\text{obs}} = 1/\tau_{\text{Li}} = \pi W_{1/2,\text{obs}} - \pi W_{1/20}$), where $W_{1/2,\text{obs}}$ and $W_{1/20}$ are the line widths (Hz) at half-height of ^7Li NMR signals with and without exchange, respectively. We used a 1.0 M LiCl/ D_2O solution as an external standard of the chemical shifts of ^7Li NMR.

3. Results and Discussion

3.1. Complex Formations of Li(I) with C211 in DEME-TfSA, EMI-TfSA, and MPP-TfSA. Figure 1 shows ^7Li NMR spectra of DEME-TfSA solutions containing LiTfSA (0.24 m, $m = \text{mol kg}^{-1}$) and C211 ($R_{\text{C211}} = [\text{C211}]/[\text{LiTfSA}] = 0.0\text{--}1.0$). One signal is found to be observed at -1.83 ppm in the DEME-TfSA solution of $R_{\text{C211}} = 0.0$. In our previous study on the structure of Li(I) in DEME-TfSA by using Raman spectroscopy,⁴⁸ the Li(I) species in DEME-TfSA was confirmed to exist as $[\text{Li}(\text{TfSA})_2]^-$ under the present experimental conditions, i.e., $[\text{LiTfSA}] = 0.24 \text{ m}$, $R_{\text{TfSA}} = ([\text{DEME-TfSA}] + [\text{LiTfSA}])/[\text{LiTfSA}] = 10.0$. Therefore, the signal at -1.83 ppm can be assigned as that due to $[\text{Li}(\text{TfSA})_2]^-$. Furthermore, it is found that a new signal is detected at -1.02 ppm and its intensity increases with an increase in R_{C211} and that in the DEME-TfSA solution of $R_{\text{C211}} = 1.0$ the signal observed at -1.83 ppm disappears and only one signal is observed at -1.02 ppm . These phenomena indicate that the signal at -1.02 ppm can be assigned to that of 1:1 complex ($[\text{Li}\cdot\text{C211}]^+$) of Li(I) with C211 and suggest that the $[\text{Li}(\text{TfSA})_2]^-$ species are complexed with C211 stoichiometrically; i.e., the stability constant (K) for $[\text{Li}(\text{TfSA})_2]^- + \text{C211} = [\text{Li}\cdot\text{C211}]^+$ in DEME-TfSA is very large. This is consistent with the facts that the C211 compound with a cavity diameter of 1.6 \AA forms a very stable complex with Li(I) (diameter = 1.56 \AA),³⁹ that the K values for the complex formation of $[\text{Li}\cdot\text{C211}]^+$ in organic solvents are very large, e.g., K (at 25°C) in methanol, ethanol, DMF, and DMSO are $10^{8.0}$, $10^{8.4}$, $10^{6.9}$, and $10^{5.8}$, respectively,⁵² and that the K values for the complex formation of Ag(I) with C222 in ILs are larger than those in DMSO.⁵³ In addition, the Popov and Lincoln groups have studied the structure of the Li(I) complex with C211 in nonaqueous solvents^{40,41} and reported that the Li(I) complex with C211 has the same inclusive structure as that in the solid state.⁵⁴ On the basis of these reports, it seems likely that the $[\text{Li}\cdot\text{C211}]^+$ complex in DEME-TfSA has the inclusive cryptate structure incorporating Li(I) into the cavity of C211.

Similar phenomena were also observed in ^7Li NMR spectra of EMI- and MPP-TfSA solutions containing

(48) Shirai, A.; Fujii, K.; Seki, S.; Umabayashi, Y.; Ishiguro, S.; Ikeda, Y. *Anal. Sci.* **2008**, *24*, 1291–1296.

(49) Bonhôte, P.; Dias, A.; Papageorgiou, N.; Kalyanasundaram, K.; Grätzel, M. *Inorg. Chem.* **1996**, *35*, 1168–1178.

(50) Sun, J.; Forsyth, M.; MacFarlane, D. R. *J. Phys. Chem. B* **1998**, *102*, 8858–8864.

(51) Lincoln, S. F. *Prog. React. Kinet.* **1977**, *9*, 1–91.

(52) Cox, B. G.; Garcia-Rosas, J.; Schneider, H. *J. Am. Chem. Soc.* **1981**, *103*, 1384–1389.

(53) Lewandowski, A.; Osinowska, M.; Stepniak, I. *J. Incl. Phenom. Macrocycl. Chem.* **2005**, *52*, 237–240.

(54) Moras, D.; Weiss, R. *Acta Crystallogr.* **1973**, *B29*, 400–403.

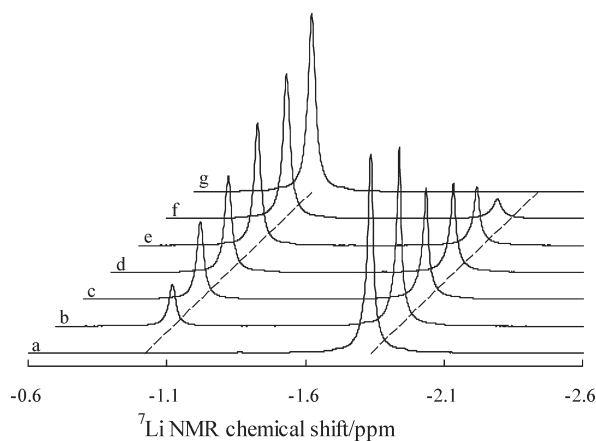


Figure 1. ^7Li NMR spectra of DEME-TFSA solutions containing LiTFSA (0.24 m) and C211. $R_{\text{C211}} = 0.0$ (a), 0.2 (b), 0.4 (c), 0.5 (d), 0.6 (e), 0.8 (f), and 1.0 (g). Temperature = 25 °C.

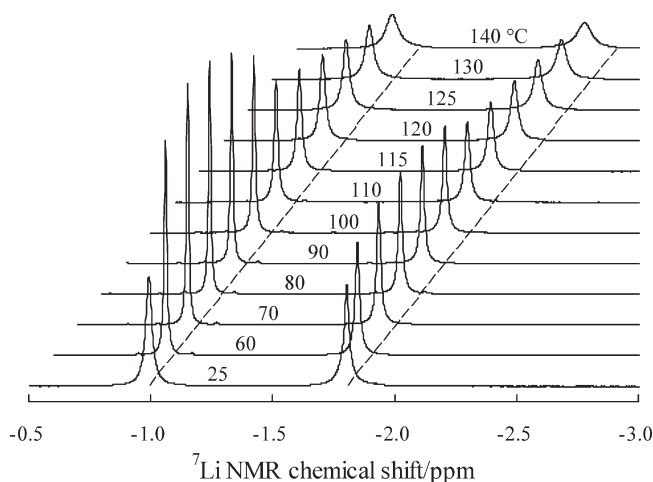


Figure 2. ^7Li NMR spectra of a DEME-TFSA solution containing LiTFSA (0.24 m) and C211 (0.12 m) measured at various temperatures. $R_{\text{C211}} = 0.5$.

LiTFSA and C211 (see Figures S6 and S7 in the Supporting Information); that is, two signals were observed at -1.82 and -1.05 ppm for the EMI-TFSA system and -1.85 and -1.04 ppm for the MPP-TFSA system, and the signals at -1.82 and -1.85 ppm disappeared in both systems of $R_{\text{C211}} = 1.0$. Furthermore, from Raman spectroscopic studies on the structures of Li(I) in EMI- and MPP-TFAS,⁵⁵ Li(I) species has been confirmed to exist as $[\text{Li}(\text{TFSA})_2]^-$.

From these results, it is proposed that, in the TFSA-based ILs containing C211 and LiTFSA, the Li(I) species exist as the complexed Li(I) ($[\text{Li}\cdot\text{C211}]^+$) and the uncomplexed Li(I) ($[\text{Li}(\text{TFSA})_2]^-$), respectively, regardless of the cationic components of ILs.

3.2. Complexation Reactions of Li(I) with C211 in DEME-TFSA, EMI-TFSA, and MPP-TFSA. Figure 2 shows the temperature dependence of ^7Li NMR spectra of the DEME-TFSA solution containing LiTFSA (0.24 m, $m = \text{mol kg}^{-1}$) and C211 (0.12 m, $R_{\text{C211}} = 0.5$), i.e., $[\text{Li}\cdot\text{C211}]^+ = 0.12$ m and $[\text{Li}(\text{TFSA})_2]^- = 0.12$ m. As

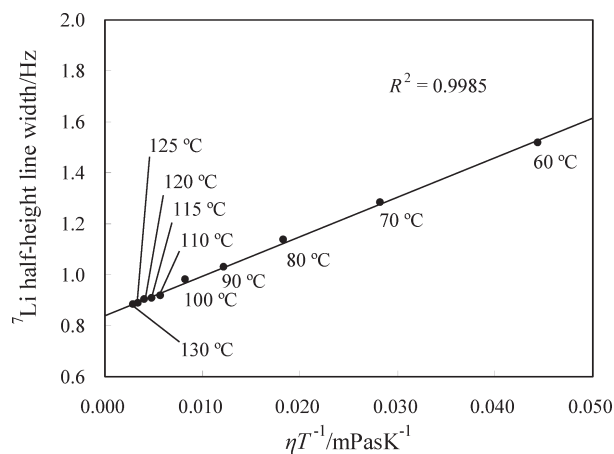


Figure 3. Plot of the line width at half-height of the ^7Li NMR signal due to $[\text{Li}\cdot\text{C211}]^+$ in the DEME-TFSA solution containing LiTFSA and C211 ($R_{\text{C211}} = 1.0$) against η/T .

seen from this figure, both signals become sharp up to 80 °C and then broad with an increase in the temperature. On the other hand, the signals of ^7Li NMR spectra for DEME-TFSA solutions of $R_{\text{C211}} = 1.0$ and 0.0 were found to be observed around -1.0 and -1.9 ppm and become sharp with an increase in the temperature from 25 to 140 °C, respectively (see Figure S8 in the Supporting Information). Hence, it is likely that the phenomena shown in Figure 2 are due to a decrease in the viscosity and the exchange of Li(I) between $[\text{Li}\cdot\text{C211}]^+$ and $[\text{Li}(\text{TFSA})_2]^-$ sites with increasing temperature. In fact, the viscosity coefficient of DEME-TFSA is 69 mPa s at 25 °C,⁵⁶ which is much larger than those of conventional nonaqueous solvents such as DMF (0.796 mPa s at 25 °C) and DMSO (1.96 mPa s at 25 °C).⁵⁷ In order to confirm the effect of the viscosity, we examined the temperature dependence of the line width at half-height ($W_{1/2}$, Hz) of the ^7Li NMR signal (Figure S8A in the Supporting Information) due to $[\text{Li}\cdot\text{C211}]^+$ in the DEME-TFSA solution of $R_{\text{C211}} = 1.0$, in which the $[\text{Li}(\text{TFSA})_2]^-$ species is not present, and hence the effect of the exchange of Li(I) on the line width should be neglected. Under this condition, the line width ($W_{1/2}$) is given by the following equations⁵⁸ because the relaxation time of ^7Li ($I = 3/2$) should be mainly controlled by the quadrupole relaxation mechanism

$$W_{1/2} = 1/\pi T_2$$

$$= 3(2I + 3)/[40\pi I^2(2I - 1)](e^2 Qq/\hbar)^2 \tau_c \quad (1)$$

$$\tau_c = CV\eta/kT + \tau_0 \quad (2)$$

where $e^2 Qq/\hbar$ is the quadrupole coupling constant, η is the viscosity of the solution, V is the molecular volume, τ_c is the correlation time, τ_0 is the correlation time at viscosity = 0, and C is the experimentally determined

(56) Zhou, Z.-B.; Matsumoto, H.; Tatsumi, K. *Chem.—Eur. J.* **2005**, *11*, 752.

(57) Riddick, J. A.; Bunger, W. B.; Sakano, T. K. *Organic Solvents, Physical Properties and Method of Purification*; Wiley: New York, 1986.

(58) Yaita, T.; Ito, D.; Tachimori, S. *J. Phys. Chem. B* **1998**, *102*, 3886–3891.

(55) Umebayashi, Y.; Mitsugi, T.; Fukuda, S.; Fujimori, T.; Fujii, K.; Kanzaki, R.; Takeuchi, M.; Ishiguro, S. *J. Phys. Chem. B* **2007**, *111*, 13028–13032.

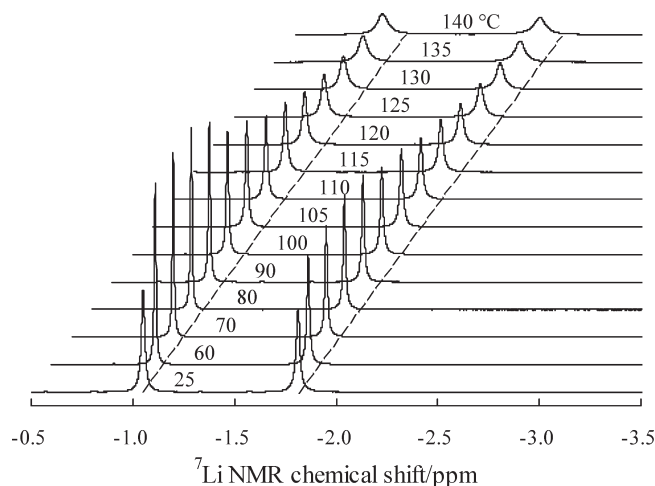


Figure 4. ^7Li NMR spectra of a EMI-TFSA solution containing LiTFSA (0.24 m) and C211 (0.12 m) measured at various temperatures. $R_{\text{C211}} = 0.5$.

dimensionless parameter. If our assumption is reasonable, a plot of $W_{1/2}$ against η/T should give a linear relationship. Figure 3 shows such a plot, where the η/T values for neat DEME-TFSA were used.²² The resulting linear relationship indicates that the sharpening of the ^7Li NMR signals in the range of 25–80 °C in Figure 2 is due to a decrease in the viscosity of DEME-TFSA. Hence, the broadening of the ^7Li NMR signals in the range of 90–140 °C should be attributed to the exchange reaction of Li(I) between $[\text{Li} \cdot \text{C211}]^+$ and $[\text{Li}(\text{TFSA})_2]^-$ sites. Moreover, both signals in Figure 2 are found to shift to lower field with an increase in the temperature. Such a lower field shift was also observed in the ^7Li NMR spectra for DEME-TFSA solutions of $R_{\text{C211}} = 1.0$ and 0.0 (see Figure S8 in the Supporting Information). These phenomena are considered to be due to changes in the bulk magnetic susceptibility (χ_v) with an increase in the temperature based on the relationship^{59,60}

$$\delta_{\text{obs(Li)}} = -\frac{4}{3}\pi\chi_v = -\frac{4}{3}\pi\chi_g\rho \quad (3)$$

where $\delta_{\text{obs(Li)}}$, χ_g , and ρ are the chemical shift of ^7Li for $[\text{Li} \cdot \text{C211}]^+$, the mass magnetic susceptibility, and the density of the sample, respectively. If $\delta_{\text{obs(Li)}}$ is dependent on only the change in χ_v of sample solutions, the plot of $\delta_{\text{obs(Li)}}$ against ρ should give a linear relationship with a slope of 2.06, because the χ_g value of neat DEME-TFSA was estimated to be $-0.491 \times 10^{-6} \text{ cm}^3 \text{ g}^{-1}$. In fact, the plot of $\delta_{\text{obs(Li)}}$ against ρ gave a linear relationship with a slope of 2.07 (see Figure S9 in the Supporting Information). Furthermore, the differences ($\Delta\delta_{\text{C-F}}$) in the chemical shifts of the signals due to $[\text{Li} \cdot \text{C211}]^+$ and $[\text{Li}(\text{TFSA})_2]^-$ in Figure 2 were found to be constant (see Figure S10 in the Supporting Information). From these results, the lower field shift observed in Figure 2 is concluded to be due to the changes in χ_v .

A similar temperature dependence was also observed in the ^7Li NMR spectra of EMI- and MPP-TFSA solutions

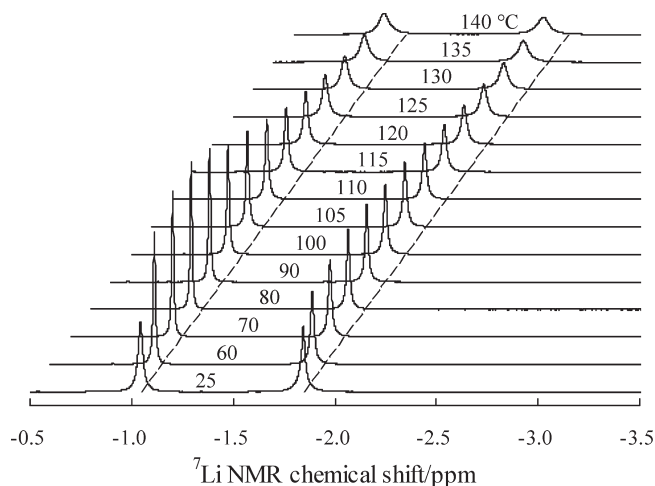
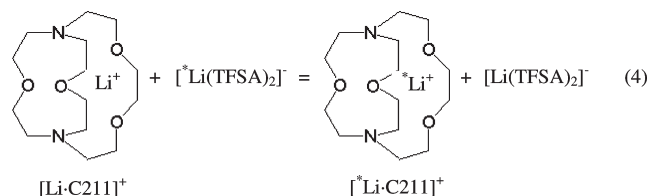


Figure 5. ^7Li NMR spectra of a MPP-TFSA solution containing LiTFSA (0.24 m) and C211 (0.12 m) measured at various temperatures. $R_{\text{C211}} = 0.5$.

containing LiTFSA (0.24 m) and C211 (0.12 m, $R_{\text{C211}} = 0.5$), as shown in Figures 4 and 5. Sharpening of the signals in the low-temperature region of these figures is also attributable to the effect of the viscosity of solutions, because the viscosity coefficients of EMI- and MPP-TFSA are also much larger than conventional nonaqueous solvents, i.e., 33 and 151 mPa s.⁶¹

From these results, it is concluded that the exchange reactions of Li(I) between $[\text{Li} \cdot \text{C211}]^+$ and $[\text{Li}(\text{TFSA})_2]^-$ sites, i.e., the complexation reactions of Li(I) with C211, occur in DEME-, EMI-, and MPP-TFSA solutions containing LiTFSA and C211.

Measurements for the exchange reactions were carried out using sample solutions (samp-1–samp-3) listed in Table 1. The apparent first-order rate constants (k_{obs}) for the exchange reactions ($\text{rate} = \tau_{\text{Li}}^{-1}[\text{Li} \cdot \text{C211}]^+ = k_{\text{obs}}[\text{Li} \cdot \text{C211}]^+$) were evaluated from $1/\tau_{\text{Li}}$ values using a two-site model of a NMR line-broadening method. The resulting k_{obs} values were plotted against the concentrations of uncomplexed Li(I) species, $[\text{Li(I)}_{\text{free}}]$ ($= [\text{Li}(\text{TFSA})_2]^- = [\text{LiTFSA}] - [\text{Li} \cdot \text{C211}]^+ = [\text{LiTFSA}] - [\text{C211}]$). The plots are found to give straight lines passing through the origin in three systems, as shown in Figures 6–8. Hence, the rate equation is expressed as $\text{rate} = k_{\text{obs}}[\text{Li} \cdot \text{C211}]^+ = k_s[\text{Li(I)}_{\text{free}}][\text{Li} \cdot \text{C211}]^+$ (k_s = second-order rate constant). This dependence of k_{obs} on $[\text{Li(I)}_{\text{free}}]$ suggests that the complexation reactions of Li(I) with C211 in DEME-, EMI-, and MPP-TFSA proceed through the following bimolecular mechanism proposed by Shcori et al.⁶²



where the asterisk is used to denote the exchange species. The k_s values were obtained from the slopes in Figures 6–8

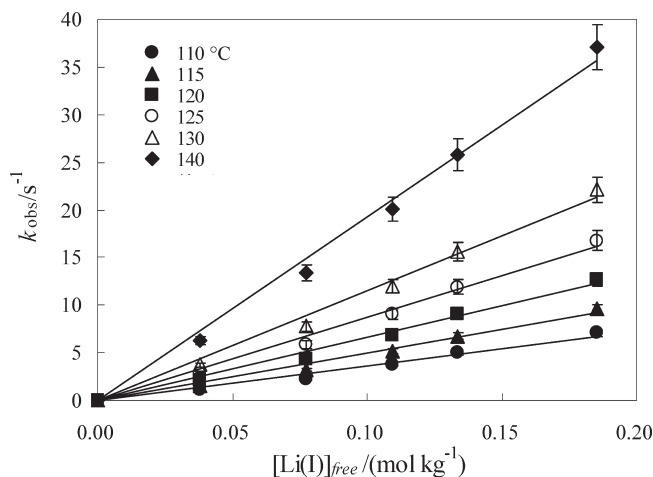
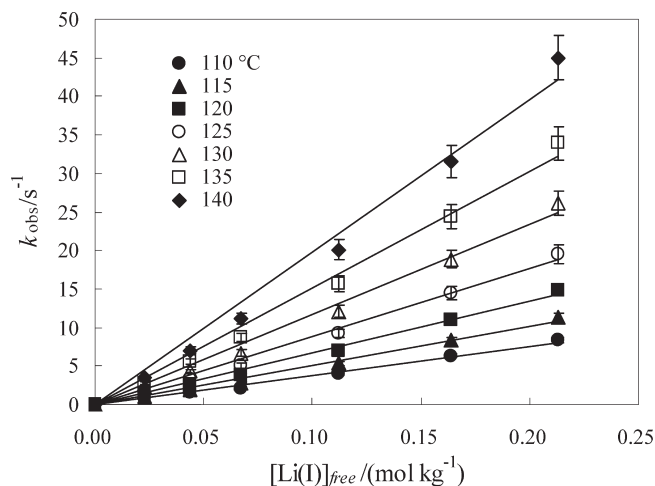
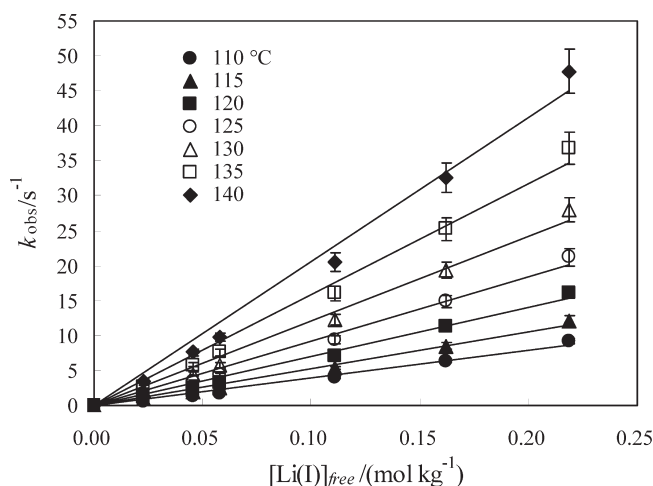
(59) Live, D. H.; Chan, S. I. *Anal. Chem.* **1970**, *42*, 791–792.

(60) Teweldemedhin, Z. S.; Fuller, R. L.; Greenblatt, M. *J. Chem. Educ.* **1996**, *73*, 906–909.

(61) Matsumoto, H.; Sakaebe, H.; Tatsumi, K. *J. Power Sources* **2005**, *146*, 45.

Table 1. Components and Water Content of Sample Solutions for Complexation Reactions of Li(I) with C211 in ILs

sample no.	ILs	[Li(I)]/m (Li salt)		R_{C211} (water content/ppm)				
samp-1	DEME-TFSA	0.24 (LiTFSA)	0.2 (10.3)	0.4 (11.6)	0.5 (12.2)	0.6 (12.9)	0.8 (14.0)	
samp-2	EMI-TFSA	0.24 (LiTFSA)	0.1 (10.1)	0.3 (11.4)	0.5 (12.7)	0.7 (14.0)	0.8 (14.6)	0.9 (15.3)
samp-3	MPP-TFSA	0.24 (LiTFSA)	0.1 (10.3)	0.3 (11.6)	0.5 (12.9)	0.7 (14.0)	0.8 (14.6)	0.9 (15.2)
samp-4	DEME-PFSA	0.20 (LiPFSA)	0.1 (7.4)	0.3 (8.5)	0.5 (9.4)	0.7 (10.4)	0.8 (10.9)	0.9 (11.5)
samp-5	DEME-HFSA	0.16 (LiHFSA)	0.3 (13.9)	0.5 (15.2)	0.9 (17.5)			

**Figure 6.** Plots of k_{obs} values against $[\text{Li(I)}]_{\text{free}}$ for the complexation reaction of Li(I) with C211 in DEME-TFSA.**Figure 8.** Plots of k_{obs} values against $[\text{Li(I)}]_{\text{free}}$ for the complexation reaction of Li(I) with C211 in MPP-TFSA.**Figure 7.** Plots of k_{obs} values against $[\text{Li(I)}]_{\text{free}}$ for the complexation reaction of Li(I) with C211 in EMI-TFSA.

and are listed in Table 2. The kinetic parameters for k_s were evaluated from the semilogarithmic plots of k_s against the reciprocal temperature (Eyring plot) and are shown in Table 3. As seen from this table (TFSA-based IL systems), the kinetic parameters are almost consistent with each other, indicating that the present complexation reactions are independent of the cationic components of ILs. This is reasonable because the Li(I) species in DEME-, EMI-, and MPP-TFSA exist as the same anionic species ($[\text{Li}(\text{TFSA})_2]^-$) and should interact with the cationic species ($[\text{Li} \cdot \text{C211}]^+$) in the same manner. This suggests that the

electrostatic interaction is important in the complexation reactions of Li(I) with C211 in the present ILs.

3.3. Complexation Reactions of Li(I) with C211 in DEME-PFSA and DEME-HFSA. According to the above mechanism, the complexation reactions of Li(I) with C211 should be affected by the anionic components of ILs because of the differences in the interactions between Li^+ and anionic species of ILs. Hence, the complexation reactions of Li(I) with C211 in DEME-PFSA and DEME-HFSA were examined. Figure 9 shows ^7Li NMR spectra of DEME-PFSA solutions containing LiPFSA (0.20 m) and C211 ($R_{C211} = 0.0\text{--}1.0$). These ^7Li NMR spectral changes are found to be very similar to those in Figures 1 and S6 and S7 in the Supporting Information. Hence, the signals at -1.03 and -1.70 ppm are assigned to be those due to the $[\text{Li} \cdot \text{C211}]^+$ complex and the Li(I) species without coordination of C211 [the uncomplexed Li(I) species], respectively. Similar ^7Li NMR spectra were observed in the DEME-HFSA solution containing LiHFSA (0.16 m) and C211 ($R_{C211} = 0.3\text{--}1.0$) (see Figure S11 in the Supporting Information). Although the structures of the uncomplexed Li(I) species in DEME-PFSA and DEME-HFSA have not been known, it seems likely that the uncomplexed Li(I) species exist as $[\text{Li}(\text{PFSA})_2]^-$ and $[\text{Li}(\text{HFSA})_2]^-$ because the structures of PFSA and HFSA are similar to that of TFSA except for the difference in the lengths of the perfluoroalkyl chains.

^7Li NMR spectra of the DEME-PFSA solution containing LiPFSA (0.20 m) and C211 (0.10 m, $R_{C211} = 0.5$) and the DEME-HFSA solution containing LiHFSA (0.16 m) and C211 (0.08 m, $R_{C211} = 0.5$) were also measured by changes in the temperature. The results are shown in Figures 10 and S12 in the Supporting Information and are

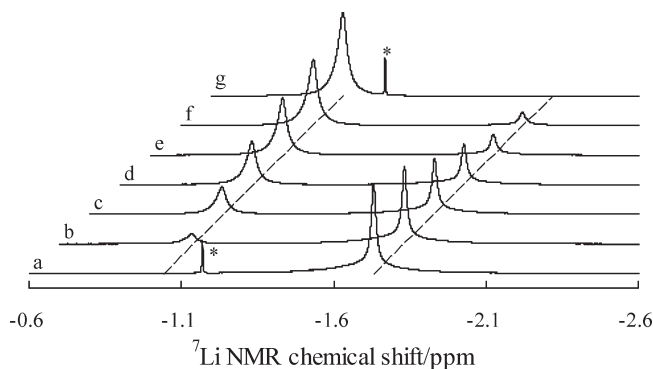
Table 2. Second-Order Rate Constants (k_s) at Various Temperatures for the Complexation Reactions of Li(I) with C211 in ILs

temp/°C	$k_s/(m^{-1} s^{-1})$				
	DEME-TFSA	EMI-TFSA	MPP-TFSA	DEME-PFSA	DEME-HFSA
110	36.4 ± 1.2	41.0 ± 1.6	37.9 ± 0.8	59.0 ± 1.2	46.7 ± 0.3
115	49.5 ± 1.5	55.2 ± 2.0	50.8 ± 1.1	77.6 ± 1.5	61.1 ± 0.4
120	66.0 ± 1.8	73.7 ± 2.4	60.7 ± 1.5	101 ± 2	79.5 ± 0.6
125	87.5 ± 2.2			131 ± 3	103 ± 1
130	115 ± 3	128 ± 4	117 ± 3	169 ± 3	133 ± 2
135		170 ± 6	151 ± 4	216 ± 4	170 ± 2
140	193 ± 4	221 ± 8	198 ± 6	284 ± 8	219 ± 4

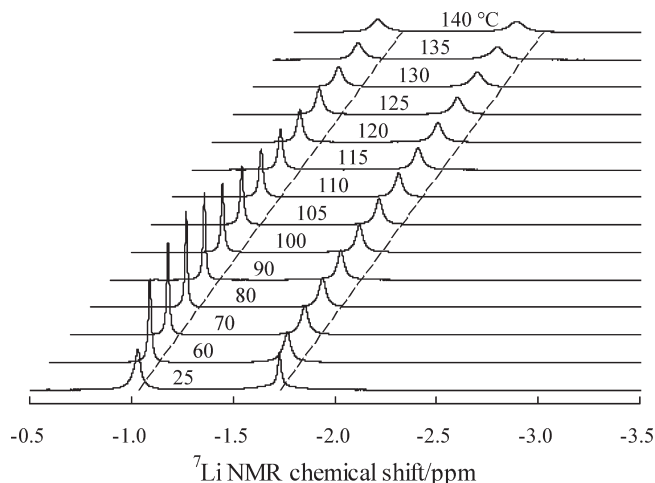
Table 3. Kinetic Parameters for the Complexation Reactions of Li(I) with C211 in ILs and Nonaqueous Solvents

system	mechanism	k_{obs}/s^{-1a}	$k_s/(m^{-1} s^{-1})^a$	$\Delta H^\ddagger/(kJ mol^{-1})$	$\Delta S^\ddagger/(J K^{-1} mol^{-1})$
DEME-TFSA	B ^b		5.57×10^{-2}	69.8 ± 0.4	-34.9 ± 1.0
EMI-TFSA	B		5.77×10^{-2}	70.6 ± 0.2	-31.9 ± 0.6
MPP-TFSA	B		6.13×10^{-2}	69.0 ± 0.3	-36.7 ± 0.7
DEME-PFSA	B		1.35×10^{-1}	65.2 ± 0.5	-43.1 ± 1.4
DEME-HFSA	B		1.14×10^{-1}	64.4 ± 0.3	-47.1 ± 0.6
DMF	D ^c	1.10×10^{-2}		68.9 ± 0.2	-51.3 ± 0.4
DMSO	D	1.13×10^{-2}		76.3 ± 0.3	-26.3 ± 0.8

^a Values at 25 °C. ^b B = bimolecular mechanism. ^c D = dissociative mechanism.

**Figure 9.** 7Li NMR spectra of DEME-PFSA solutions containing LiPFSA (0.20 m) and C211. $R_{C211} = 0.0$ (a), 0.1 (b), 0.3 (c), 0.5 (d), 0.7 (e), 0.9 (f), and 1.0 (g). Temperature = 25 °C. *: 7Li NMR signal of a D_2O solution containing $LiCF_3SO_3$ (0.1 m; external standard).

found to be similar to those shown in Figures 2, 4, and 5. This indicates that the Li(I) species exchange between $[Li \cdot C211]^+$ and $[Li(PFSA)_2]^-$ or $[Li(HFSA)_2]^-$ sites. Kinetic analyses were carried out using sample solutions (samp-4 and samp-5) of Table 1 in a manner similar to that mentioned above. Figure 11 shows the plots of k_{obs} against $[Li(I)_{free}]$ ($= [Li(X)_2^-]$ ($X = PFSA$ or $HFSA$) $= [LiX] - [C211]$) at various temperatures. The k_s values were obtained from the slopes of Figure 11 and are listed in Table 2. Their kinetic parameters were also obtained from the semilogarithmic plots of k_s against the reciprocal temperature and are summarized in Table 3. As seen from Table 3, the kinetic parameters for the DEME-PFSA and DEME-HFSA systems are different from those for the DEME-, EMI-, and MPP-TFSA systems, especially their k_s values are about 2 times larger than those in the DEME-, EMI-, and MPP-TFSA systems. These results indicate that the anionic components of ILs affect the complexation reaction as expected. However, the effect cannot be explained by the difference in the lengths of the perfluoroalkyl chains in TFSA, PFSA, and HFSA because the k_s values increase in the order of the following IL systems: DEME-PFSA >

**Figure 10.** 7Li NMR spectra of a DEME-PFSA solution containing LiPFSA (0.20 m) and C211 (0.10 m) measured at various temperatures. $R_{C211} = 0.5$.

DEME-HFSA > DEME-TFSA. The detailed information on the structures of Li(I) species in DEME-PFSA and DEME-HFSA must be necessary to discuss the effect of the anionic components of the present ILs on the complexation reactions of Li(I) with C211.

3.4. Complexation Reactions of Li(I) with C211 in Nonaqueous Solvents. The complexation reactions of Li(I) with C211 in DMF and DMSO were examined to compare with the corresponding reactions in ILs mentioned above because the chemical forms of the Li(I) species in the solutions prepared by dissolving LiTFSA into DMF and DMSO should be different from those of the Li(I) species in TFSA-based ILs, i.e., $[Li(TFSA)_2]^-$. Salomon et al. have reported that the association constants (K_a) for LiTFSA and $LiClO_4$ in CH_3CN are 4.73 and 16.5, respectively.^{63,64} Furthermore, the studies on

(63) Croce, F.; D'Aprano, A.; Baujundias, C.; Koach, V. R.; Walker, C. W.; Salomon, M. *J. Electrochem. Soc.* **1996**, *143*, 154–159.
 (64) Salomon, M. *J. Solution Chem.* **1993**, *22*, 715–725.

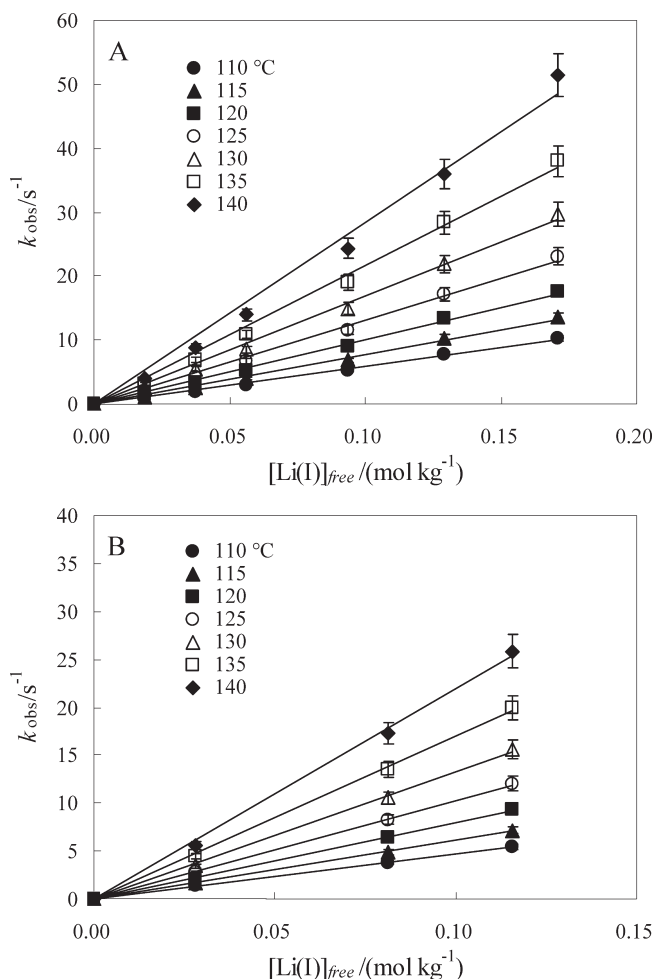


Figure 11. Plots of k_{obs} values against $[\text{Li(I)}]_{\text{free}}$ for the complexation reactions of Li(I) with C211 in DME-PFSA (A) and DME-HFSA (B).

the association of LiClO_4 in DMF using Raman and ^7Li and ^{13}C NMR^{65–67} suggest that Li(I) species are not associated with TFSA but solvated by DMF or DMSO ($[\text{Li}(\text{solvent})_n]^+$). The stability constants for the complex formation of Li(I) with C211 in DMF and DMSO are known to be $10^{6.9}$ and $10^{5.8}$ at 25 °C, respectively.⁵² Hence, the Li(I) species in DMF or DMSO containing LiTFSA and C211 are considered to exist as $[\text{Li} \cdot \text{C211}]^+$ and $[\text{Li}(\text{solvent})_n]^+$. Figure 12 shows the ^7Li NMR spectra of a DMF solution containing LiTFSA (0.24 m) and C211 (0.12 m, $R_{\text{C211}} = 0.5$) measured at various temperatures. From comparison with ^7Li NMR spectra for DMF solutions of $R_{\text{C211}} = 0.0$ and 1.0 (see Figure S13 in the Supporting Information), the signals at 0.47 and -0.56 ppm were assigned to be due to the solvated Li(I) and the $[\text{Li} \cdot \text{C211}]^+$ species, respectively. Two peaks are found to become broad with an increase in the temperature. This phenomenon is similar to those in ^7Li NMR spectra for Li(I) exchange reactions in a DMF solution containing LiClO_4 (0.25 m) and C211 (0.25 m).³⁹ Hence, the ^7Li NMR spectral changes in Figure 12 are

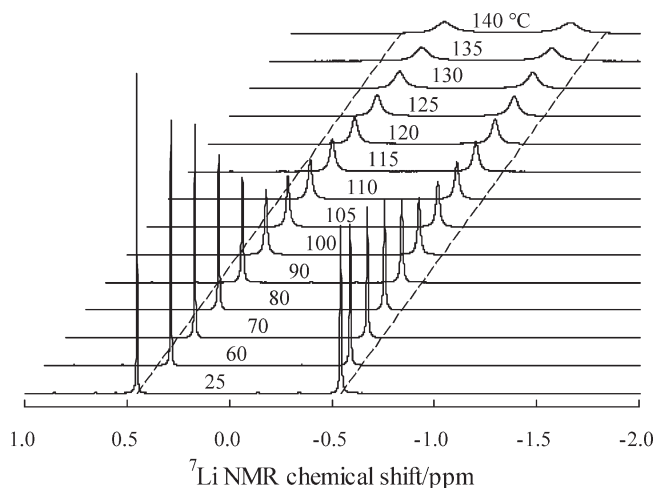
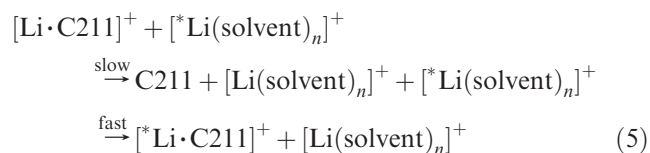


Figure 12. ^7Li NMR spectra of a DMF solution containing LiTFSA (0.24 m) and C211 (0.12 m) measured at various temperatures. $R_{\text{C211}} = 0.5$. The chemical shifts of ^7Li were determined using a D_2O solution containing 0.10 M LiCl as an external reference.

Table 4. Apparent First-Order Rate Constants (k_{obs}) at Various Temperatures for the Complexation Reactions of Li(I) with C211 in DMF or DMSO

temp/°C	$k_{\text{obs}}/\text{s}^{-1}$					
	R_{C211} (DMF system)			R_{C211} (DMSO system)		
	0.1	0.5	0.9	0.1	0.5	0.9
110	6.66	6.80	6.75	12.6	13.3	12.5
115	8.90	9.14	8.98	17.2	18.4	16.5
120	11.7	12.1	11.8	23.9	24.9	
125	15.2	16.0	15.4	32.3	33.8	
130	20.0	20.9	19.7	44.6	45.6	
135	26.0	27.2	25.4	62.0	61.9	

considered to be attributed to the exchange reaction of Li(I) between $[\text{Li} \cdot \text{C211}]^+$ and $[\text{Li}(\text{DMF})_n]^+$ sites. Similar phenomena were also observed in a DMSO solution containing LiTFSA (0.24 m) and C211 (0.12 m, $R_{\text{C211}} = 0.5$) (see Figure S14 in the Supporting Information). The k_{obs} values for DMF or DMSO solutions with various R_{C211} were obtained and are listed in Table 4. As seen from this table, the k_{obs} values are constant without depending on the components of sample solutions. These results are consistent with those of Popov et al.,⁴⁰ indicating that the exchange reactions of Li(I) between $[\text{Li} \cdot \text{C211}]^+$ and $[\text{Li}(\text{solvent})_n]^+$ (solvent = DMF or DMSO) sites proceed through the following dissociative mechanism.



The kinetic parameters for k_{obs} were evaluated from the semilogarithmic plots of k_{obs} against the reciprocal temperature and are listed in Table 3. These kinetic parameters are found to be in fair agreement with those for DMF or DMSO solutions containing C211 and LiClO_4 , that is, $1.30 \times 10^{-2} \text{ s}^{-1}$, $64.5 \pm 2.5 \text{ kJ mol}^{-1}$, and $-64.8 \pm 5.9 \text{ kJ K}^{-1} \text{ mol}^{-1}$ for DMF and $2.32 \times 10^{-2} \text{ s}^{-1}$, $64.5 \pm 2.5 \text{ kJ mol}^{-1}$, and $-57.8 \pm 5.9 \text{ kJ K}^{-1} \text{ mol}^{-1}$ for DMSO.³⁹

(65) James, D. W.; Mayes, R. E.; Leong, W. H.; Jamil, I. M.; Zhen, G. *Faraday Discuss. Chem. Soc.* **1988**, 85, 269–281.

(66) Cahen, Y. M.; Handy, P. R.; Roach, E. T.; Popov, A. I. *J. Phys. Chem.* **1975**, 79, 80–85.

(67) Berman, H. A.; Stengle, T. R. *J. Phys. Chem.* **1975**, 79, 1001–1005.

From these results, it is proposed that the complexation reactions in ILs proceed in a manner different from those in conventional nonaqueous solvents. The difference in the reaction mechanism is explained by those in the chemical forms of the uncomplexed Li(I) species in ILs and nonaqueous solvents, that is, $[\text{Li}(\text{solvent})_n]^+$ in nonaqueous solvents and $[\text{Li}(\text{X})_2]^-$ in ILs. The approach of positively charged species ($[\text{Li}(\text{solvent})]^+$) to $[\text{Li}\cdot\text{C211}]^+$ in DMF or DMSO should be more difficult than that of the negatively charged species ($[\text{Li}(\text{TFSA})_2]^-$, $[\text{Li}(\text{HFSA})_2]^-$, and $[\text{Li}(\text{HFSA})_2]^-$) to $[\text{Li}\cdot\text{C211}]^+$ in ILs. This is considered to cause the differences in the reaction mechanism in nonaqueous solvents and ILs.

4. Conclusion

We measured ^7Li NMR spectra of DEME-TFSA, EMI-TFSA, MPP-TFSA, DEME-PFSA, and DEME-HFSA solutions containing LiX (X = TFSA, PFSA, or HFSA) and C211 at various temperatures. As a result, it was found that the Li(I) species in these IL solutions can form a 1:1 complex ($[\text{Li}\cdot\text{C211}]^+$) with C211 stoichiometrically, that the Li(I) species exchange between $[\text{Li}\cdot\text{C211}]^+$ and the uncomplexed Li(I) ($[\text{Li}(\text{X})_2]^-$) sites through the bimolecular mechanism $[\text{Li}\cdot\text{C211}]^+ + [\text{Li}(\text{X})_2]^- = [\text{Li}\cdot\text{C211}]^+ + [\text{Li}(\text{X})_2]^-$, and that the Li(I) exchange reactions are not affected by the cationic components but anionic ones in ILs. Furthermore, ^7Li NMR spectra of DMF and DMSO solutions containing C211 and LiTFSA were measured at various temperatures. It was found that the Li(I) species exist as $[\text{Li}\cdot\text{C211}]^+$ and $[\text{Li}(\text{solvent})_n]^+$ (solvent = DMF or DMSO) in these solutions and that the exchange reactions of Li(I) between $[\text{Li}\cdot\text{C211}]^+$ and $[\text{Li}(\text{solvent})_n]^+$ sites occur via the dissociative mechanism. The differences in the reaction mechanisms between ILs and nonaqueous solvents were attributed to

those in the chemical forms of the uncomplexed Li(I) species; i.e., the negatively charged species ($[\text{Li}(\text{X})_2]^-$) in ILs can more easily approach the $[\text{Li}\cdot\text{C211}]^+$ complex than the positively charged species ($[\text{Li}(\text{solvent})_n]^+$) in nonaqueous solvents.

From these results, it is concluded that interactions between the anionic components of ILs and the positively charged metal complexes or ions are the important factor for controlling the complex formation reactions in ILs. This is consistent with the results of Eldik et al. and our previous study.

Acknowledgment. The authors are thankful to Dr. H. Miyashiro, Dr. Seki, and Y. Ohno of Central Research Institute of Electric Power Industry for their kind support.

Supporting Information Available: ^1H , ^{13}C , and ^{19}F NMR spectra of DEME-TFSA, EMI-TFSA, MPP-TFSA, DEME-PFSA, and DEME-HFSA (Figures S1–S5), ^7Li NMR spectra of EMI-TFSA solutions containing LiTFSA (0.24 m) and C211 (Figure S6), ^7Li NMR spectra of MPP-TFSA solutions containing LiTFSA (0.24 m) and C211 (Figure S7), ^7Li NMR spectra of DEME-TFSA solutions of $R_{\text{C211}} = 1.0$ (A) and 0.0 (B) measured at various temperatures (Figure S8), a plot of the ^7Li NMR chemical shift ($\delta_{\text{obs(Li)}}$) against ρ (Figure S9), a plot of $\Delta\delta_{\text{C-F}}$ against temperature (Figure S10), ^7Li NMR spectra of DEME-HFSA solutions containing LiHFSA (0.16 m) and C211 (Figure S11), ^7Li NMR spectra of DEME-HFSA solutions containing LiHFSA (0.16 m) and C211 (0.08 m) measured at various temperatures (Figure S12), ^7Li NMR spectra of DMF solutions containing LiHFSA (0.24 m) and C211 (Figure S13), and ^7Li NMR spectra of DMSO solutions containing LiTFSA (0.24 m) and C211 (0.12 m) measured at various temperatures (Figure S14). This material is available free of charge via the Internet at <http://pubs.acs.org>.